Characterization of a Novel Model of Overuse-Induced Calcific Achilles Tendinopathy in Mice: Contralateral Tendinopathy Following Unilateral Tenotomy

Liang Wang, MD[a,b,1], Jie Zhang, MD[a,b,1], Gang-hui Yin MD[a,b,1] , Zhong-min Zhang, MD[a,b], Tian-yu Chen, MM[a,b], Jian Jin, MM[b,d], Ping-lin Lai, PhD[a,b,c], Bin Huang, MD[a,b] Bo Yan, MD[a,b], Yu-hui Chen, MM[a,b], Da-di Jin, MD[a,b,*] , Min-jun Huang, MD[a,b,*]

[a]Department of Orthopedics, the Third Affiliated Hospital of Southern Medical University, Guangzhou 510665, Guangdong, PR China

[b]Academy of Orthopedics. Guangdong Province, Guangzhou 510665, Guangdong, PR China

[c]Department of Cell Biology, School of Basic Medical Science, Southern Medical University, Guangzhou 510515, Guangdong, PR China

[d]Department of Spine Surgery, Nanfang Hospital, Southern Medical University, Guangzhou 510515, Guangdong, PR China

Correspondence to Dr Da-di Jin, Department of Orthopaedic, the Third Affiliated Hospital of Southern Medical University, 183 West Zhongshan Avenue, Guangzhou 510665, China. T: +86-20-38252295; F: +86-20-38252295; E-mail: jindadi@yahoo.cn. or Dr. Minjun Huang, Academy of Orthopaedics. Guangdong Province, 183 West Zhongshan Avenue, Guangzhou 510630 China. T: +86-20-62784308; F:+86-20-62784288; E-mail: hmjlceb@163.com

[1] Liang Wang, Jie Zhang and Gang-hui Yin equally contributed to this work.

Abstract

Objective. To develop a simple but reproducible overuse induced animal model of Achilles tendinopathy in mice for better understanding the underlying mechanism and prevention of calcific Achilles tendinopathy.

Methods. 80 C57/B6 mice (8-9 weeks old) were employed and randomly divided into control group and experimental group. Unilateral Achilles tenotomy was performed on the right hindlimb of experiment group. After 12 weeks, the onset of Achilles tedinopathy in the contralateral Achilles tendon was determined by radiological assessment, histological analysis, electron microscopy observation and biomechanical test.

Results. The onset of calcific Achilles tendinopathy in contralateral Achilles tendon was confirmed after 12 weeks unilateral tenotomy. The contralateral Achilles tendon of experimental group was characterized as hypercelluarity, neovascularization and fused collagen fiber disarrangement, compared to the control group. Importantly, intratendon endochondral ossification and calcaneus deformity was featured in contralateral Achilles tendon. Additionally, poor biomechanical properties in the contralateral Achilles tendon revealed the incidence of Achilles tedinopathy.

Conclusion. We hereby introduce a novel simple but reproducible spontaneous contralateral calcific Achilles tendinopathy model in mice, which represents the overuse conditions during the tendinopathy development in human-beings. It should be a useful tool to further study the underlying pathogenesis of calcific Achilles tendinopathy.

Introduction

Achilles tendinopathy is a significant clinical disease featured by activity-related pain, focal movement limitation and intratendinous imaging changes with high prevalence in elite athletes and active population[1]. However, the treatment of Achilles tendinopathy was mainly based on theoretical rationale and clinical experience due to its unclear underlying pathogenesis[2]. Despite recent studies have recommended the Achilles tendon degeneration (tendinosis) is typical histopathological appearance during the pathogenesis of tendinopathy[3-5], its pathophysiology, the very foundation of the treatment decision, is not fully understood. On account of potential demand to further indentify the efficiency of medical intervention, validated animal models with Achilles tendinopathy should be developed to represent the consistent conditions and known risk factors in human[6]. Thus, several animal models of Achilles tendinopathy have been established in the previous studies. Sullo *et al* administered weekly injections of PGE1 into the Achilles tendons of rats for 5 weeks to induce Achilles tendon tendinosis[7]. Moreover, Glazebrook *et al* recently employed an uphill treadmill rat model to develop Achilles tendinopathy[8]. Interestingly, Nakagawa *et al* reported a disuse model with tail suspension on rats for five weeks resulted in a decrease in collagen fiber surface area and an increase in proportion of thin to thick collagen fibers in Achilles tendon[9].

Even though existed studies shed light on the novel established models of Achilles tendinopathy, they do have distinct drawbacks such as complex inducible conditions and special treadmill instrument requirement, confounding variables interference,

which may compromise its reproducible characterization and restrict its applications[10-12]. Therefore, the established animal model with more simple and high reproducible design could gain more popularity in consistent with the increasing clinical interest of Achilles tendinopathy.

In addition, since the aberrant activated differentiation of tendon-derived stem cells (TDSCs) have been supposed as a trigger of tendinopathy development, its erroneous chondrogenic and osteogenic differentiation may contribute to terminal calcific Achilles tendinopathy[13]. But the underlying mechanisms and its prevention are still poorly understood because of the absence of suitable animal model up to now. An excellent *in vivo* model will be beneficial to better understanding the underlying pathophysiology of tenocyte differentiation.

Herein, we introduce a novel Achilles tendinopathy model in mice characterized by simple procedure but highly reproducible. In this model, the disorganization of collagen fibers, neovascularity, hypercelluarity, endochondral ossification and poor Achilles tendon mechanical properties have been indentified, proven to be a successful establishment of the calcific Achilles tendinopathy.

Materials and methods

Animal experiment

The Animal Care and Use Committee of Southern Medical University approved all animal experimental protocols, which followed the principles expressed in the National Institute of Health Guide. Eighty male C57/B6 mice (8–9 weeks old) were obtained from the experimental animal research center of Southern Medical

University. The animals were randomly divided into 2 groups (n = 40). All of the mice were anesthetized with a mixture of ketamine (90 mg/kg, i.p.) and xylazine (10 mg/kg, i.p.), and then the experimental group underwent midpoint Achilles tenotomy on left hindlimbs through a posterior approach under aseptic condition. Incision was routinely closed with an interrupted 4-0 silk suture, whilst the control group underwent skin incision only. The mice were kept in the standard condition. At 12 weeks post-operation, all animals were sacrificed by administration of a fatally high dose of anesthetics. The right Achilles tendon tissues from soleus muscle attachment to calcaneus insertional endpoint were harvested.

Scanning electron microscopy (SEM) observation

The Achilles tendon tissues were longitudinally incised directly, and then the specimens were fixed in 2.5 % glutaraldehyde for 12 hours. They were dehydrated in a graded acetone series and critical-point-dried in carbon dioxide. After this procedure, specimens were cut into 0.5 cm × 1.0 cm pieces, fixed onto a scanning electron microscopy (SEM) stub, and sputter-coated with gold of approximately 20 nm. The images of the specimens were captured by SEM (Hitachi, S-3000N, Japan) in high vacuum mode with accelerating voltages of 10-20 kV.

Transmission electron microscopy (TEM) observation

The Achilles tendon tissue were dissected and immediately fixed in 2.5% glutaraldehyde for 1h, rinsed three times in 0.1 M sodium cacodylate buffer (pH 7.4) and re-fixed in 2% osmium oxide in 0.1 M cacodylate buffer for 2 h, then washed three times in distilled water. After that, the specimens were stained with ethanolic

111 uranyl acetate overnight and then rinsed in distilled water, dehydrated in graded
112 concentrations of ethanol series at 4 ℃. The Achilles tendons were embedded with
113 propylene oxide in a fresh mixture of Epon and ethanol, and polymerized for 2 days at
114 60 ℃. Thin 50–70 nm thickness sections were cut along the longitudinal axis of the
115 tendon with a diamond knife mounted on an ultra microtome (Meyco-Diatome,
116 Switzerland) and placed on electron microscope grids. Sections on the grids were
117 stained with 2% uranyl acetate and lead citrate solution and viewed in a transmission
118 electron microscope(Hitachi, H600, Japan) operated at an accelerating voltage of 80
119 kV. The fibril diameters were measured, and the distribution was analyzed.

120 **Histological analysis**

121 The pictures of gross examination for Achilles tendons were documented once the
122 animals were sacrificed and limbs skinned. The Achilles tendons were isolated and
123 fixed in 4% neutral-buffered paraformaldehyde overnight, followed by decalcified in
124 EDTA(0.5M, PH=7.4) at 4 ℃ for 2 weeks. Serially dehydration in graded ethanol and
125 paraffin embedding were subsequently conducted. The blocks were cut into 4-μ
126 m-thick sections. Hematoxylin-eosin （H&E）staining and Toluidine-blue staining
127 were then accomplished. The celluarity and vascularity has been calculated as
128 previously described[4,14].

129 For immunohistochemical（IHC）staining to evaluate the endochondral ossification in
130 the degenerated Achilles tendons, paraffin-embedded sections were deparaffinated
131 and rehydrated through graded ethanol. Endogenous peroxidase activity was blocked
132 with 0.3% hydrogen peroxide in PBS. Then the sections were blocked with 5% horse

serum albumin and incubated with the primary antibody of collagen II (1:100 dilution; Abcam, USA) and collagen X(1:100 dilution; Abcam, USA) at 4℃ overnight. The sections were washed with PBS for three times and then incubated with secondary anti-mouse IgG for 1 h at 37℃. The colorization developed in 3, 30-diaminobenzidine tetrachloride solution.

For immunofluorescence(IF) staining, paraffin-embedded samples were deparaffinated and rehydrated in graded ethanol and water. After washing with PBS, sections were blocked with 5% horse serum for 30 min at room temperature and then incubated with mouse anti-Collagen Ⅲ polyclonal antibody (1:100) (Abcam, USA) overnight at 4℃. After washing with PBS, sections were incubated with Alexa Fluor 594 goat anti mouse immunoglobulin G (ZSGB-Bio, China) for 30 min. Finally, slides were washed and mounted with prolong gold antifade reagent (Invitrogen, USA). The images were captured by confocal laser scanning microscopy (Olympus FV1000, Japan)

Radiological analysis

All animals were assessed by X-ray analysis to detect imaging changes in Achilles tendons at 12 weeks after tenotomy. When the animals were sacrificed, the hindlimbs were amputated from knee joint for the micro-CT assessment (ZKKS-MCT-Sharp-III scanner, Caskaisheng, CHINA). The scanning system was set to 70kV, 30W, and 429μA. The 3 dimensional reconstruction of hindlimbs was conducted by 3DMed 2.2 software. The ossification or mineralization in Achilles tendons was indentified as the Region Of Interest (ROI).

155 **Biomechanical analysis**

156 Tensile loading tests were performed on an Instron 5843 tensile tester (Instron, USA).
157 The Right Achilles tendons with calcaneus were harvested at 12 weeks after tenotomy
158 and stored in PBS at – 80°C. The cross-sectional area was assessed by measuring the
159 thickness in three points along the tendon's length. Then the tendons with calcaneus
160 have been firmly fixed into clamps of the tensile tester and kept moist in PBS during
161 the experiments. The tendons were stretched with a constant strain rate. The
162 displacement and force has been recorded until the Achilles tendons break in the
163 midpoint. The failure tensile load and the stiffness of Achilles tendon were then
164 calculated.

165 **Statistical analysis**

166 Data analysis was performed with SPSS 13.0. The results were presented as the mean
167 ± SD. Two-sample t-tests were used for data analysis. P values < 0.05 were
168 considered statistically significant.

169 **Results**

170 **Hypercelluarity, neovascularization in the contralateral Achilles tendon after 12**
171 **weeks unilateral tenotomy**

172 Since hypercelluarity and neovascularization in tendon are common characters of
173 tendinosis or tendinopathy[15], we firstly evaluated the potential changes in the
174 contralateral Achilles tendon by H&E staining after 12 weeks unilateral tenotomy.
175 Compared to control, there were increased and disorganized tenocytes inside the
176 contralateral Achilles tendon. A large mount of vascular were infiltrated in the

177 contralateral Achilles tendon (Fig.1). These results indicated that the contrallateral
178 Achilles tendon could be hypercelluar and hypervascular after 12 weeks unilateral
179 tenotomy, which implies the underlying tendinosis or tendinopathy incidence.

180 **Fiber disarrangement and collagen fusion in the contrallateral Achilles tendon**
181 **after 12 weeks unilateral tenotomy**

182 To comprehensively assess the microstructure of contralateral Achilles tendinopathy,
183 we next performed both the SEM and TEM observation. The longitudinal collagen
184 fiber disorganization was found in contralateral Achilles tendon versus control. There
185 were more fused collagen fibers in the contralateral Achilles tendon with higher fiber
186 diameter. Moreover, micro-gaps between fiber collagens were commonly observed
187 (Fig.2). Interestingly, the ossification lesions with chondrocyte-like cells and
188 neovasculars were detected inside the contralateral Achilles tendon compared to
189 control (Fig.3), which could further contribute to the fiber collagen fusion and
190 disorientation. These results confirmed the contralateral Achilles tendinopathy after
191 12 weeks unilateral tenotomy.

192 **Mineralization in the contralateral Achilles tendon and calcaneus deformity after**
193 **12 weeks unilateral tenotomy**

194 To further evaluate the mineralization in the contralateral Achilles tendon, we
195 examined and reconstructed the contralateral hindlimb using X-ray and micro-CT
196 scanning. The ossifications were apparently detected in the both ends of contralateral
197 Achilles tendon, which were mainly cortex bones with bone marrow cavity, whilst no
198 ossification was detected in the control group. What's more, in the experimental group,

199 calcaneus deformity was presented in the reconstructed 3-dimension images. There
200 were bony callus surround the calcaneus insertion of contralateral Achilles tendon. On
201 the contrary, no calcaneus malformation was shown in the control group(Fig.4). These
202 results strongly suggested mineralization was developed in the contralateral Achilles
203 tendon, which is the most important feature of calcific Achilles tendinopathy.

204 **Fibrocartilage metaplasia and endochondral ossification in the contralateral**
205 **Achilles tendon after 12 weeks unilateral tenotomy**

206 To investigate the underlying mechanism of ossification in the contralateral Achilles
207 tendon, we performed H&E and toluidine blue staining. The results showed a large
208 number of chondrocyte-like cells were presented inside the ossification area of
209 Achilles tendon and calcaneus (Fig.5), which implied endochondral ossification may
210 be involved in this process. Consequently, collagen II, collagen Ⅹ IHC staining were
211 conducted to identify endochondral ossification, both of which play a crucial role in
212 endochondral ossification. There were abundant collagen II and collagen Ⅹ-positive
213 cells inside both the ossification area of Achilles tendon and calcaneus, conversely
214 rare positive cells were determined in the control group (Fig.6). In addition, IF
215 staining confirmed that more collagen Ⅲ expression in the tenocytes of experimental
216 group versus control, which indicated the achilles tendinosis in the experimental
217 group(Fig.6). These results suggested that ossification of the contralateral Achilles
218 tendon is cell-mediated endochondral ossification. Fibrocartilage metaplasia from
219 either tenocyte stem cells or bone marrow stem cells could be the initial step of
220 endochondral ossification in Achilles tendon enthesis.

Poor biomechanical properties in contralateral Achilles tendon after 12 weeks unilateral tenotomy

In general, Achilles tendinopathy results in poor biomechanical properties, which is considered the main reason for Achilles tendon rupture under normal loading[16]. We achieved the biomechanical analysis of contralateral Achilles tendon and recorded the maximal failure tensile loading and the stiffness of contralateral Achilles tendon. The cross-sectional area was decreased slightly in the experimental group. The maximal failure tensile loading in the experimental group was significantly reduced while the stiffness was significantly increased in the experimental group compared to control group(Table.1). The biomechanical properties changes may result from the ossification development and collagen fiber disorganization in the Achilles tendon. In summary, these results delineated the significant biomechanical properties loss in the contralateral Achilles tendon after 12 weeks unilateral tenotomy, which is the essential feature of Achilles tendinopathy.

Discussion

Calcific Achilles tendinopathy is a common and significant disease in elite athletes and older, sedentary and overweight individuals[17]. The aetiopathogenesis and treatment of this disease remains controversial[18], which gives rise to more interests in developing better animal models to address the gap in our understanding of calcific Achilles tendinopathy. Although unilateral Achilles tenotomy has been widely employed as a trauma-induced heterotopic ossification model in the previous studies[19-21], the changes of contralateral Achilles tendon in this model has not been

243 reported. In the present study, we found the spontaneous contralateral Achilles
244 tendinopathy after unilateral transection of Achilles tendon in mice, which could be a
245 novel calcific Achilles tendinopathy model.
246 Compared to the existing animal models for Achilles tendinopathy investigation, our
247 model has several benefits: firstly, the model of contralateral calcific Achilles
248 tendinopathy is quite simple but highly reproducible which can be created only with
249 the unilateral Achilles tendon transection. Non-special instrument is required, while
250 some particular machines such as running-mills and pneumatic pistons[5,8,11,12], are
251 generally necessary in the existing models. Secondly, it will be beneficial for imitating
252 the natural pathogenesis of calcific tendinopathy in the contralateral Achilles tendons
253 without any additional intervention. Furthermore, since this model has been
254 established in mice, it is possible to take advantage of existing transgenic mice to
255 investigate the pathogenesis of Achilles tendinopathy. With this model, the genetic
256 predispostion of Achilles tendinopathy could be reconsidered instead of poorly
257 understood.
258 Understanding the main pathophysiology underlying Achilles tendinopathy is the core
259 to develop mechanism-based animal models[22]. Currently, there is still a long way to
260 go before we comprehensively delineate the mechanism of calcific Achilles
261 tendinopathy, however, overuse has generally been supposed as a critical extrinsic
262 factor of Achilles tendinopathy[23]. Thus, several overuse-induced animal models of
263 tendinopathy have been established [5,8,24]. In the present study, unilateral Achilles
264 tendon transection leads to dysfunction of the injury tendon, subsequently, the

equilibration of mechanical loading has been broke on contralateral Achilles tendon, where more stress loading are bearing while standing. To some extent, the contralateral Achilles tendon will encounter overuse. The overload stress induces the micro-injury of tendon to accelerate the degeneration of contralateral Achilles tendon. With time going by, unbalanced homeostasis in contralateral tendon will aggravate the Achilles tendinopathy subsequently. These results also strongly suggest that the contralateral Achilles tendon could not be indentified as the valid control of the unilateral tenotomy model in mice.

Interestingly, the morphological character of calcaneus has been remodeled in this model. From the results of Micro-CT analysis, the deformity of calcaneus has been detected, especially in the insertional region of Achilles tendon. The bony callus mass emerges in the posterosuperior area of calcaneus. The histological assessment indentify the fibrocartilaginous callus, woven bone and laminar bone with bone marrow cavity are located in the interface of the Achilles tendon enthesis. These results indicated the endochondral ossification is involved in the process of calcific Achilles tendinopathy, which is consistent with the study conducted by Lin et al in rats[25]. Consequently, we proposed calcaneus stress fracture could play an important role via endochondral ossification during calcific Achilles tendinopathy. The mechanical overload on the contralateral hindlimb induces stress fracture of calcaneus and increasing tensile loading of Achilles tendon results in calcaneus avulsion fracture where micro-fracture and micro-repair may occur coincide. Therefore, the calcaneus has been remodeling through endochondral ossification during the fracture healing.

The secondary blood vessel invasion into the tendon and potential fibrocartilage metaplasia form the tendon fibroblast may further contribute to the calcific deposition or ossification in the Achilles tendon. From this model, it is notable that calcaneus and Achilles tendon should be deemed to be a functional unit. The calcaneus fracture especially in the insertion of Achilles tendon may trigger subsequent calcific Achilles tendinopathy, which indicated the prevention of insertional Achilles tendinopathy should be taken into consideration during the treatment of calcaneus avulsion fracture or stress fracture treatment. Active precaution for calcaneus stress fracture may confer benefit to Achilles tendinopathy prevention.

Additionally, a solitary ectopic ossification is detected in the enthesis of soleus muscle from micro-CT analysis, indicating the erroneous chondral differentiation of tendon derived stem cells in the Achilles tendon may be involved. It has been proposed the formation of calcific deposits in calcifying tendinopathy is chondrocyte-mediated[26], which has also been demonstrated in histological analysis of this study. With mechanical loading overuse, the erroneous differentiation of TDSCs to chondrocyte and osteoblast could compromise the normal tendon healing, leading to weaken properties and activity-related pain[27]. Hence, the redirection of TDSCs differentiation to tendoncyte has been supposed to be a novel treatment target for Achilles tendinopathy[28]. Nevertheless, the underlying pathogenesis of aberrant TDSCs differentiation is not fully understood at the moment, which may restrict development of effective or evidence-based therapy strategy. Therefore, through by the model, it will facilitate our better understanding on the pathogenesis of TDSCs

309 erroneous differentiation in the calcific Achilles tendinopathy, consequently
310 encouraging a novel perspective for its treatment.
311 However, there are some drawbacks to this model indeed. Lack of internal control
312 may result in overlook of the individual variance. It is important that the animal
313 model should provide reproducible results that consistent with human conditions.
314 When it refers to the Achilles tendinopathy in sedentary population, which means
315 disuse or underuse of Achilles tendon, this model is not suitable. In addition, taking
316 account of the crosstalk within the bilateral Achilles tendon and the existing evidence
317 from bench and bedside, further studies should look into either the potential effect of
318 sympathetic nerve modulation or endocrine predisposing factors in this model.
319 In conclusion, we hereby introduce a novel simple but reproducible spontaneous
320 contralateral calcific Achilles tendinopathy model in mice, which represents the
321 overuse conditions during the tendinopathy development in human-beings. It should
322 be a useful tool to further study the underlying pathogenesis of calcific Achilles
323 tendinopathy, including endochondral ossification from cancalneus stress fracture and
324 the erroneous differentiation of TDSCs.

325 **Conflict of Interests statement**

326 The authors declare no conflicts of interest.

327 **Acknowledgements**

328 This research was supported by grants from National Natural Sciences Foundation of
329 China (31271271, 31228007, 81260401 and 81171764). We also thank Lu Tang and
330 Aihong Yang for excellent technical assistance.

Author contributions

All authors were involved in drafting the article or revising it critically for important intellectual content, and all authors approved the final version to be published. Dr. Dadi Jin and Dr. Xiaochun Bai had full access to all of the data in the study and takes responsibility for the integrity of the data and the accuracy of the data analysis.

Study conception and design. Dadi Jin, Xiaochun Bai, Liang Wang, Minjun Huang.

Acquisition of data. Liang Wang, Minjun Huang, Zhongmin Zhang, Tianyu Chen, Jian Jin, Xiaochen Zheng, Bin Huang, Bo Yan, Yuhui Chen, Shengfa Li.

Analysis and interpretation of data. Liang Wang, Minjun Huang, Pinglin Lai.

Manuscript preparation. Liang Wang, Minjun Huang, Dadi Jin, Xiaochun Bai.

References

1. Zafar MS, Mahmood A, Maffulli N. Basic science and clinical aspects of achilles tendinopathy. Sports Med Arthrosc 2009;17:190-7.

2. Abbassian A, Khan R. Achilles tendinopathy: pathology and management strategies. Br J Hosp Med (Lond) 2009;70:519-23.

3. Silva RD, Glazebrook MA, Campos VC, Vasconcelos AC. Achilles tendinosis: a morphometrical study in a rat model. Int J Clin Exp Pathol 2011;4:683-91.

4. Cho NS, Hwang JH, Lee YT, Chae SW. Tendinosis-like histologic and molecular changes of the Achilles tendon to repetitive stress: a pilot study in rats. Clin Orthop Relat Res 2011;469:3172-80.

5. Ng GY, Chung PY, Wang JS, Cheung RT. Enforced bipedal downhill running induces Achilles tendinosis in rats. Connect Tissue Res 2011;52:466-71.

353 6. Warden SJ. Animal models for the study of tendinopathy. Br J Sports Med
354 2007;41:232-40.
355 7. Sullo A, Maffulli N, Capasso G, Testa V. The effects of prolonged peritendinous
356 administration of PGE1 to the rat Achilles tendon: a possible animal model of chronic
357 Achilles tendinopathy. J Orthop Sci 2001;6:349-57.
358 8. Glazebrook MA, Wright JR Jr, Langman M, Stanish WD, Lee JM. Histological
359 analysis of achilles tendons in an overuse rat model. J Orthop Res 2008;26:840-6.
360 9. Nakagawa Y, Totsuka M, Sato T, Fukuda Y, Hirota K. Effect of disuse on the
361 ultrastructure of the achilles tendon in rats. Eur J Appl Physiol Occup Physiol
362 1989;59:239-42.
363 10. Dirks RC, Warden SJ. Models for the study of tendinopathy. J Musculoskelet
364 Neuronal Interact 2011;11:141-9.
365 11. Heinemeier KM, Skovgaard D, Bayer ML, Qvortrup K, Kjaer A, Kjaer M, et al.
366 Uphill running improves rat Achilles tendon tissue mechanical properties and alters
367 gene expression without inducing pathological changes. J Appl Physiol
368 2012;113:827-36.
369 12. Andersson G, Forsgren S, Scott A, Gaida JE, Stjernfeldt JE, Lorentzon R, et al.
370 Tenocyte hypercellularity and vascular proliferation in a rabbit model of tendinopathy:
371 contralateral effects suggest the involvement of central neuronal mechanisms. Br J
372 Sports Med 2011;45:399-406.
373 13. Rui YF, Lui PP, Chan LS, Chan KM, Fu SC, Li G. Does erroneous differentiation
374 of tendon-derived stem cells contribute to the pathogenesis of calcifying tendinopathy?

375 Chin Med J (Engl) 2011;124:606-10.

376 14. Aström M, Rausing A. Chronic Achilles tendinopathy. A survey of surgical and
377 histopathologic findings. Clin Orthop Relat Res 1995;316:151-64.

378 15. Cook JL, Feller JA, Bonar SF, Khan KM. Abnormal tenocyte morphology is more
379 prevalent than collagen disruption in asymptomatic athletes' patellar tendons. J Orthop
380 Res 2004;22:334-8.

381 16. Hess GW. Achilles tendon rupture: a review of etiology, population, anatomy, risk
382 factors, and injury prevention. Foot Ankle Spec 2010;3:29-32.

383 17. Oliva F, Via AG, Maffulli N. Physiopathology of intratendinous calcific deposition.
384 BMC Med. 2012;10:095-104.

385 18. Alfredson H, Cook J. A treatment algorithm for managing Achilles tendinopathy:
386 new treatment options. Br J Sports Med 2007;41:211-6.

387 19. McClure J. The effect of diphosphonates on heterotopic ossification in
388 regenerating Achilles tendon of the mouse. J Pathol 1983;139:419-30

389 20. Lin L, Shen Q, Leng H, Duan X, Fu X, Yu C. Synergistic inhibition of
390 endochondral bone formation by silencing Hif1α and Runx2 in trauma-induced
391 heterotopic ossification. Mol Ther 2011;19:1426-32.

392 21. Lin L, Chen L, Wang H, Wei X, Fu X, Zhang J. Adenovirus-mediated transfer of
393 siRNA against Runx2/Cbfa1 inhibits the heterotopic ossification in animal model.
394 Biochem Biophys Res Commun 2006;349:564-72

395 22. Warden SJ. Development and use of animal models to advance tendinopathy
396 research. Front Biosci 2009;14:4588-97.

397 23. Wilder RP, Sethi S. Overuse injuries: tendinopathies, stress fractures,
398 compartment syndrome, and shin splints. Clin Sports Med 2004;23:55-81
399 24. Nakama LH, King KB, Abrahamsson S, Rempel DM. Evidence of tendon
400 microtears due to cyclical loading in an in vivo tendinopathy model. J Orthop Res
401 2005; 23:1199-205.
402 25. Lin L, Shen Q, Xue T, Yu C.Heterotopic ossification induced by Achilles
403 tenotomy via endochondral bone formation: expression of bone and cartilage related
404 genes. Bone 2010; 46:425-31
405 26. Maffulli N, Reaper J, Ewen SW, Waterston SW, Barrass V. Chondral metaplasia in
406 calcific insertional tendinopathy of the Achilles tendon. Clin J Sport Med
407 2006;16:329-34.
408 27. Zhang J, Wang JH. Mechanobiological response of tendon stem cells: implications
409 of tendon homeostasis and pathogenesis of tendinopathy. J Orthop Res
410 2010;28:639-43.
411 28. Lui PP, Chan KM. Tendon-derived stem cells (TDSCs): from basic science to
412 potential roles in tendon pathology and tissue engineering applications. Stem Cell Rev
413 2011;7:883-97
414
415
416
417
418

419

420 **Table 1: Biomechanical parameters of Achilles tendon complex**

Group	Control(n=8)	Experimental(n=8)	p Value
Cross-sectional area (mm^2)	0.29 ± 0.03	0.32 ± 0.04	0.08
Failure tensile load (N)	13.02 ± 0.86	8.35 ± 0.58	0.00
Stiffness (N/mm)	25.79 ± 2.01	32.00 ± 2.52	0.00

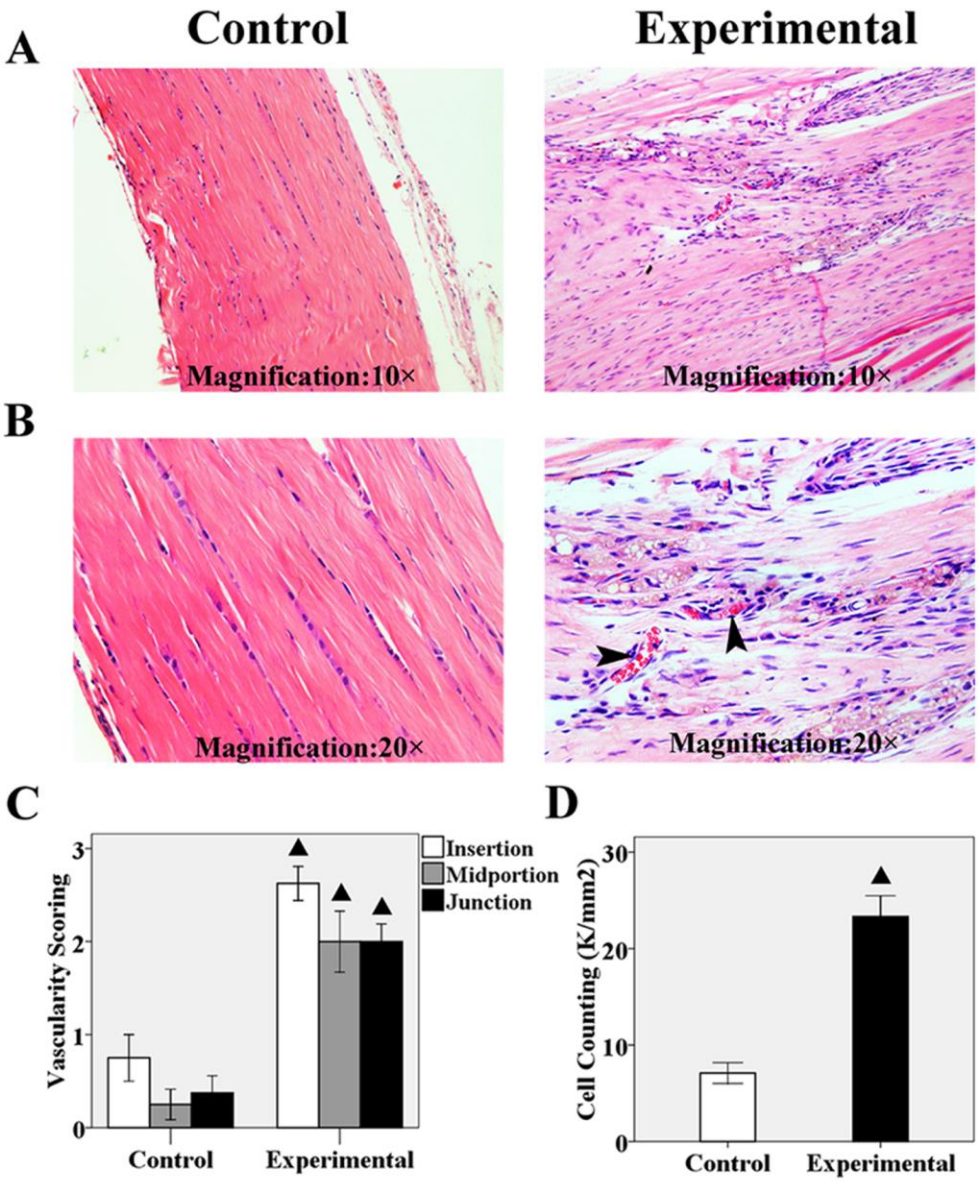

Figure 1. Hypercelluarity, neovascularization in the contralateral Achilles tendon after 12 weeks unilateral tenotomy. **A and B,** Representative H&E staining of Achilles tendon in experimental and control group. The hypercelluarity, fiber disorganization and neovascularization (shown with black arrows) was detected in the experimental group compared to control group**. C,** The vascularity scoring of experimental group in three portion of Achilles tendon was significant increased compared to the control group. **D,** The Achilles tenocytes counting of experimental group was significant more than control group. ▲ represent the comparison with control group, $P < 0.05$.

421

422

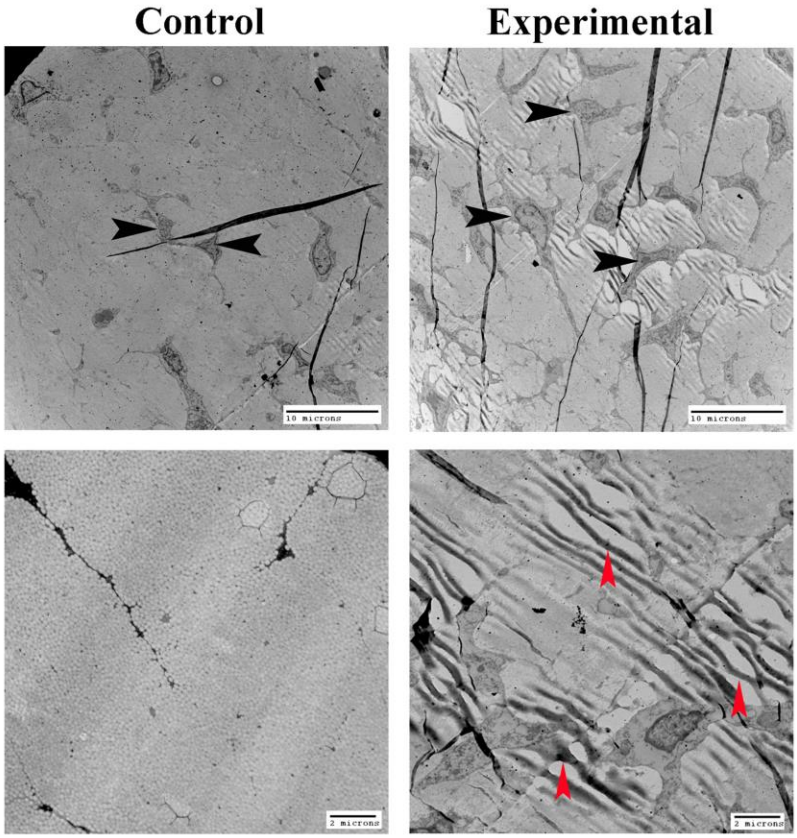

Figure 2. Representative Achilles tendon transmission electron microscopy observation. The longitudinal collagen fiber disorganization was found in ontralateral Achilles tendon versus control. There are micro-gaps between collagen fibers in the experimental group. Fibers with higher diameters (sh-own with red arrows) were presented in the experimental group compared to control group. More tenocytes (shown with black arrows) were located in the experimental group.

423

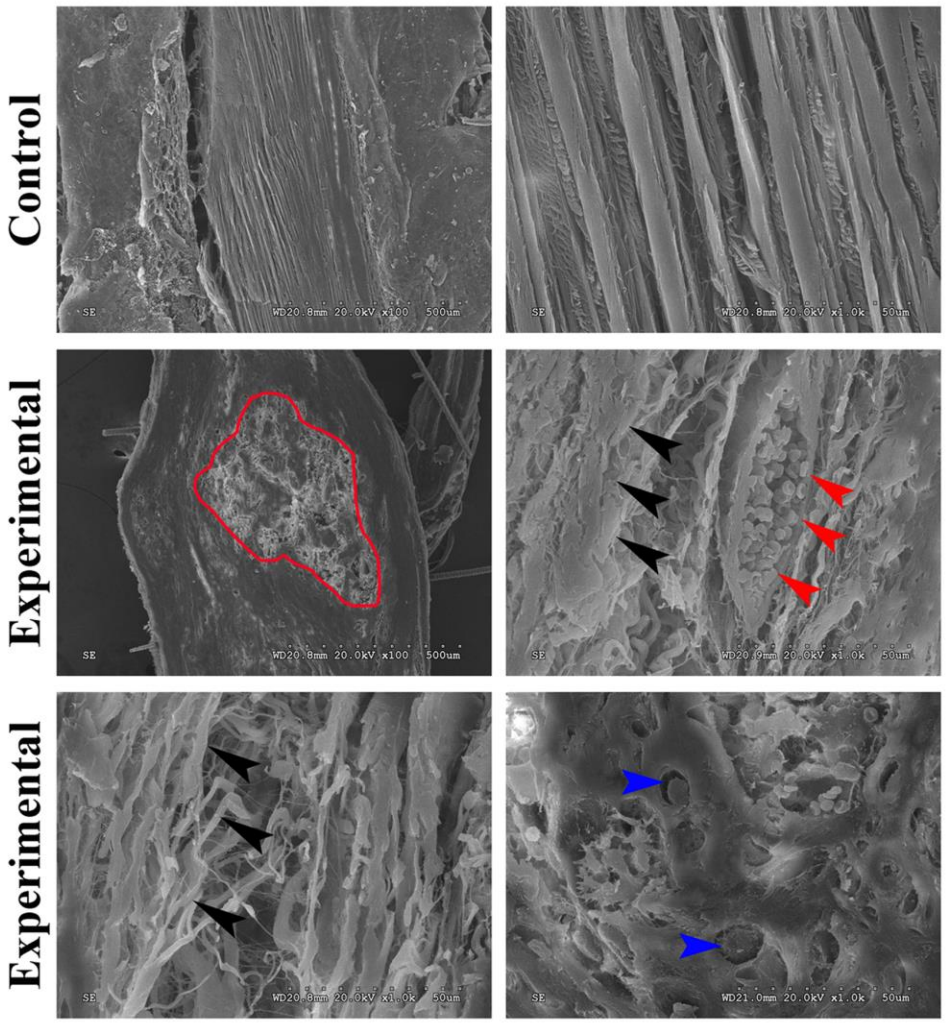

Figure 3. Representative Achilles tendon scanning electron microscopy observation. A ectopic ossification lesion (delineated by red line) was shown in the experimental Achilles tendon, chondrocytes-like cells with regular lacuna (shown with blue arrows) has been detected in the ossification area. New vascular growth (shown with red arrows) into Achilles tendon and longitudinal disoriented collagen fibers (shown with black arrows) was also demonstrated in the experimental group.

424

425

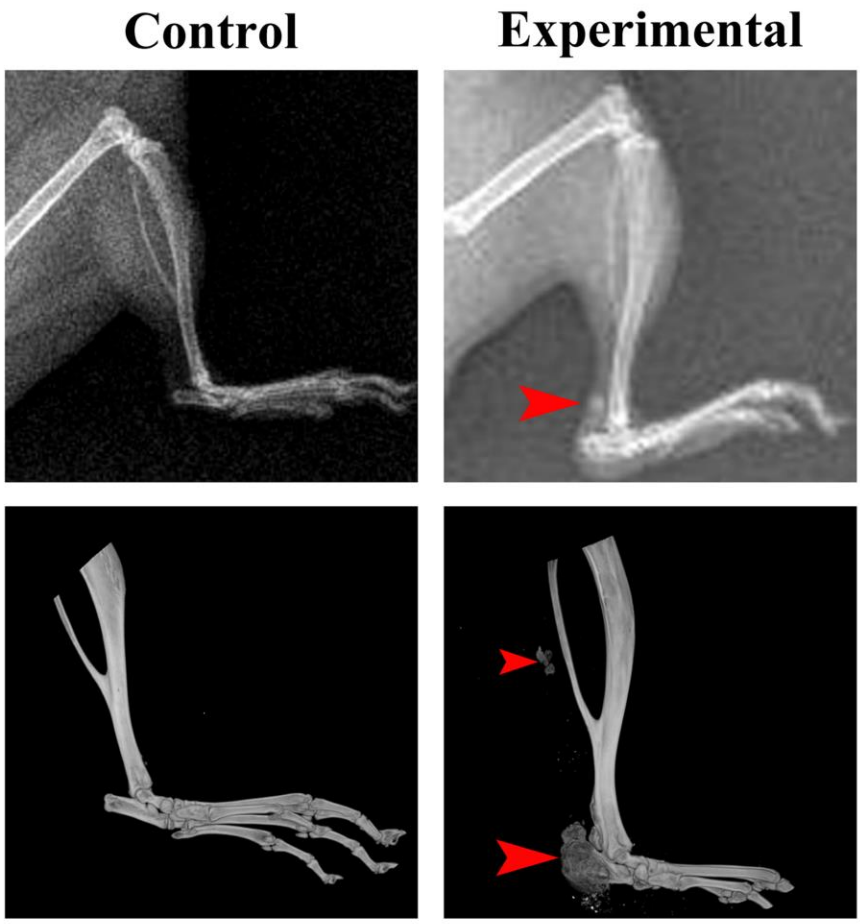

Figure 4. Representative observation of X-ray examination and micro-CT scanning for Achilles tendon of experimental group. A high density shadow of Achilles tendon in the experimental group has been detected by X-ray examination (shown with red arrows). Normal calcaneus shape was obscure from the X-ray plain film. Calcaneus deformity and Achilles tendon mineralization have been presented in the experimental group compared to control group by micro-CT three dimensional reconstruction.

426
427

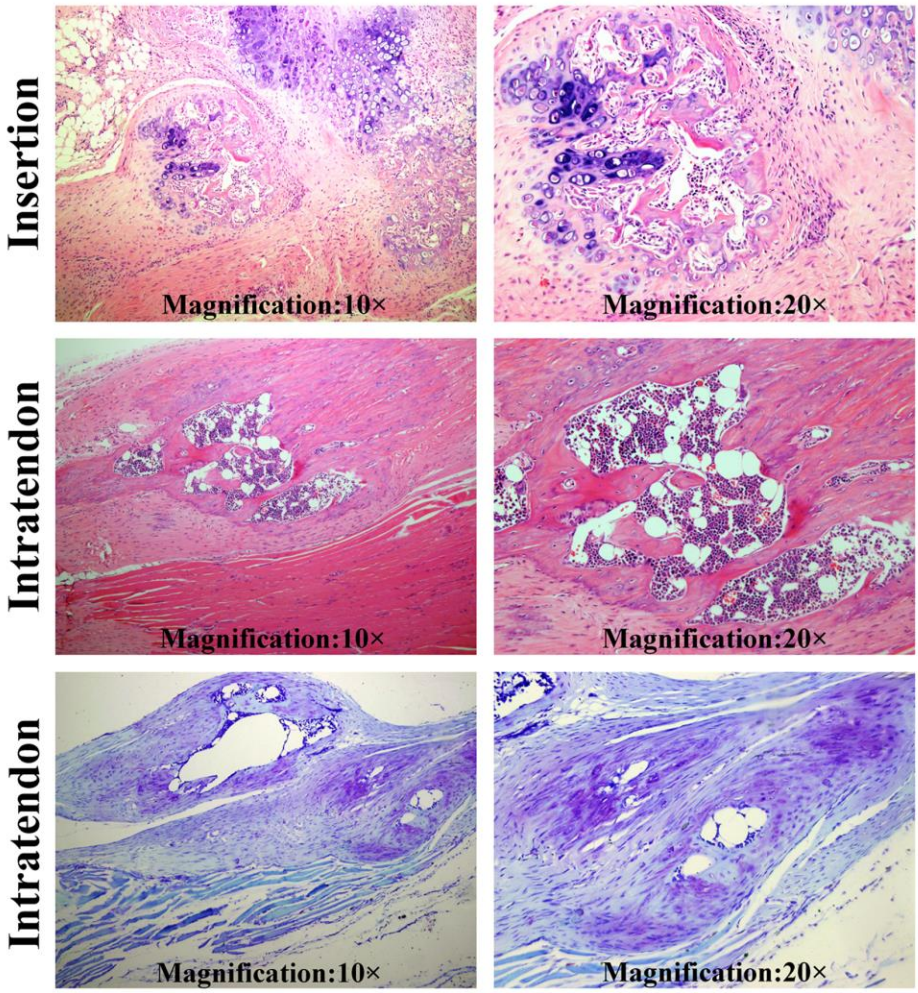

Figure 5. Fibrocartilage metaplasia and endochondral ossification in the contralateral Achilles tendon after 12 weeks unilateral tenotomy. Fibrocartilage metaplasia in the calcaneus insertion of experimental group has been found. Hypertrophic chondrocyte-like cells were distributed in the calcaneus and Achilles tendon in the experimental group. A mature cortex bone with bone marrow cavity has been detected intra the Achilles tendon. Ossification with specific stained chondrocytes intra Achilles tendon has been shown by toluidine-blue staining in experimental group.

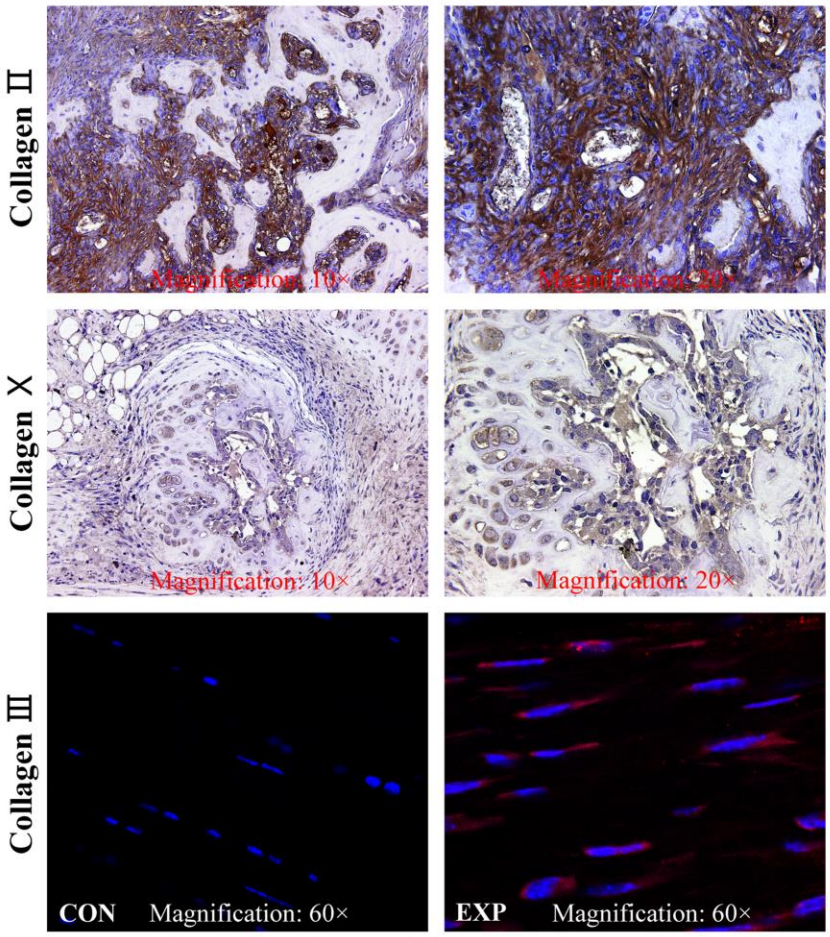

Figure 6. Representative IHC and IF staining for collagen protein expression in the experimental group. Collagen Ⅱ and collagen Ⅹ protein has been expressed in the ossification area. Large number of positive-stained cells presented in the ossification area of Achilles tendon and calcaneus. Collagen Ⅲ expression by tenocytes in experimental group was detected in the Non ossification area of Achilles tendon compared to control group.